Reduction of defect-induced ferromagnetic stability in passivated ZnO nanowires*

Wu Fang(吴 芳)[a)†], Meng Pei-Wen(孟培雯)[b)], Luo Kang(罗 康)[b)], Liu Yun-Fei(刘云飞)[b)], and Kan Er-Jun(阚二军)[c)]

[a)] School of Science, Nanjing Forestry University, Nanjing 210037, China
[b)] College of Information Science and Technology, Nanjing Forestry University, Nanjing 210037, China
[c)] Key Laboratory of Soft Chemistry and Functional Materials (Ministry of Education), and Department of Applied Physics, Nanjing University of Science and Technology, Nanjing 210094, China

(Received 16 July 2014; revised manuscript received 15 October 2014; published online 30 January 2015)

First-principles calculations are performed to study the electronic structures and magnetic properties of ZnO nanowires (NM). Our results indicate that the single Zn defect can induce large local magnetic moment ($\sim 2\mu_B$) in the ZnO NWs, regardless of the surface modification. Interestingly, we find that local magnetic defects have strong spin interaction, and favor room-temperature ferromagnetism in bared ZnO NW. On the other hand, although H passivation does not destroy the local magnetic moment of Zn vacancy, it does greatly reduce the spin interaction between magnetic defects. Therefore, our results indicate that H passivation should be avoided in the process of experiments to maintain the room-temperature ferromagnetism.

Keywords: vacancy, magnetic interaction, ZnO nanowires, DFT calculations

PACS: 75.50.Pp, 71.15.Mb, 71.55.Gs, 75.10.–b **DOI:** 10.1088/1674-1056/24/3/037504

1. Introduction

Recently, dilute magnetic semiconductors (DMSs) have attracted broad interest due to their potential applications in spintronic devices, which can utilize both the charge and spin of electrons.[1–3] One of the important problems in this research field is how to search for an ideal DMS with ferromagnetism at or above the room temperature for practical applications. Traditionally, the magnetic moments in a DMS have been introduced by the doping magnetic elements, which contain partially 3d or 4f subshells.[4–7] However, the clusters or secondary phases of the magnetic impurities are comparatively easy to form due to the presence of magnetic elements in the host semiconductor, and are difficult to be avoided.

On the other hand, whether the observed ferromagnetism in this kind of DMS comes from the doping magnetic elements is still under debate. Interestingly, in recent years, room-temperature ferromagnetism (RFM) has been achieved in the un-doped wide bandgap d^0 semiconductors, e.g., ZnO, HfO_2, SnO_2, MgO, In_2O_3, TiO_2, and CaO, or doped with the light elements such as H, C, N, K, Li, and Mg.[8–20] In contrast from DMS, there are no magnetic ions in the host materials. Consequently, it is quite interesting to explore the possible origin of the observed magnetism. Unfortunately, the origin of the magnetism in these materials is still controversial, although most studies have shown that the cationic defects may be the possible origin,[21,22] there are still many works suggesting that anionic vacancies may be the key to produce magnetism. For example, recently, we have theoretically explored if anionic vacancies can also produce magnetic states in some semiconductors.[23]

Although previous theoretical works have reported that vacancies induce the intrinsic magnetic properties, we still do not know how the surface changes the magnetic properties in such semiconductors. Xiang *et al.* predicted that the RFM in the DMS is very sensitive to superficial hydrogen passivation and magnetic interactions can be significantly enhanced.[24] The essential reason for these interesting phenomena has not yet been found. Thus it is interesting for us to study whether such effects also exist in d^0 semiconductors as well.

Here we choose ZnO nanowire (NW) as the main prototype materials for the so-called "d^0 semiconductor" because of the successful growth of the ZnO NW network and various electronic or photonic devices proposed in recent experiments.[25–27] To this aim, the ZnO NW has been considered as a typically technological material for the novel electronic and optical equipments, such as transparent electrodes for solar cells,[28] field-effect transistors,[29] light-emitting device,[30] and electricity nanogenerators.[31] ZnO NW also has potential applications in future nano spintronics because it can possess both semiconducting and magnetic properties at the same time. Based on recent theoretical and experimental evidence, it has been suggested that the intrinsic defects may

*Project supported by the National Natural Science Foundation of China (Grant Nos. 11474165, 21203096, and 11204137), the Natural Science Foundation of Jiangsu Province, China (Grant Nos. BK20130031, BK20131420, and BK2012392), and the Fundamental Research Funds for the Central Universities of China (Grant No. 30920130111016).

†Corresponding author. E-mail: fangwu@mail.ustc.edu.cn

© 2015 Chinese Physical Society and IOP Publishing Ltd

play an important role in the magnetic origin of ZnO NW. In the present work, the electronic structures and magnetic properties of ZnO nanowires with Zn vacancies are systematically studied via first-principle calculation to explore the surface effect on the magnetic interaction.

2. Computational methods

All of our calculations are performed within the framework of a spin-polarized density functional theory (DFT) as implemented in the Vienna Ab initio Simulation Package (VASP)[32] and the generalized gradient approximation (GGA) exchange–correlation functional.[33] As we know, the GGA has been well used to describe the magnetic properties in d^0 semiconductors. The interaction between valence electrons and ion cores is described by the projected augmented wave (PAW) method.[34,35] In this simulation, the NW axis is along the c direction. To ensure a negligible interaction between two neighbor NWs, they are each separated by a vacuum gap of ~ 20 Å. The convergence in energy is set to 10^{-5} eV for self-consistent field calculations and that of the force in geometry optimization is set to 0.01 eV/Å. In the case of the defect-free and the single defected NWs, we use a $1\times1\times2$ supercell, and $1\times1\times4$ supercell is applied for the research on the magnetic interactions between the two Zn defects in the NWs. A $1\times1\times3$ k-mesh with the Monkhorst–Pack k-point scheme is adopted.

3. Results and discussion

Here we mainly focus on the ZnO NWs with hexagonal cross sections along the [0001] direction with a diameter about 1 nm, as shown in Figs. 1(a) and 1(b). Pseudohydrogen is used to saturate the dangling bonds of the NW surface to get H-passivated ZnO NWs. A side view of the bared and passivated NWs is presented in Figs. 1(c) and 1(d). In order to research the magnetic origin in ZnO NWs, the electronic and magnetic properties of the single cationic vacancy and double cationic vacancies in ZnO NWs are systematically carried out via first principles for both bared and passivated ZnO NWs. For comparison, the electronic and magnetic properties of the defect-free ZnO NWs are also performed in this work.

The calculated lattice constant c in defect-free ZnO NW is about 5.2054 Å, which is in good agreement with experimental values, and the lattice constants of the defected NWs are fixed to this value since the Zn defect changes only marginally the lattice constant. To probe the origin of the different nature of magnetism in both of bared and passivated NWs, we plot the density of state (DOS) in Fig. 2. As shown in Figs. 2(a) and 2(b), both bared and passivated NWs are found to be nonmagnetic semiconductors and the band gap is about 1.3 eV and 2.3 eV, respectively. The results suggest that the passivated NW's band gap increases due to the annihilation of surface states in bared NW.

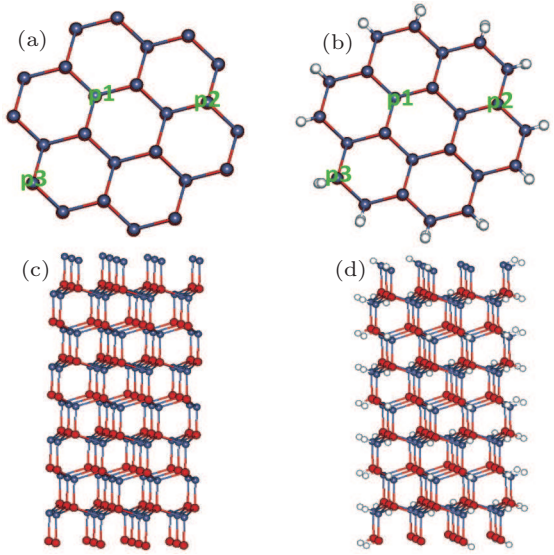


Fig. 1. (color online) (a) Top view of a bared ZnO NW with a diameter about 1.0 nm. (b) Top view of a ZnO NW passivated by pseudo-H atoms. (c) Side view of a bared ZnO NW. (d) Side view of a passivated ZnO NW with a $1\times1\times4$ supercell. p1, p2, and p3 in (a) and (b) denote three inequivalent Zn positions.

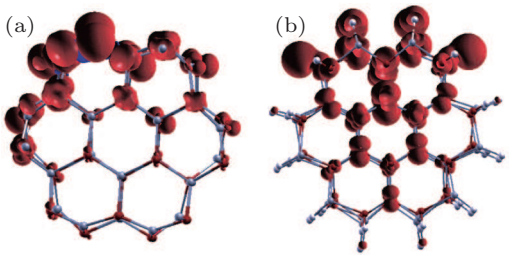


Fig. 2. (color online) Spin density of (a) bared and (b) H-passivated ZnO NWs with single Zn vacancy. The spin density is much more localized in H-passivated ZnO NM than that in bared ZnO NW.

For single cationic vacancy in ZnO NWs, there are three different configurations (p1, p2, and p3 in Figs. 1(a) and 1(b) denote three inequivalent Zn positions). To identify the most stable defected position, we calculate the formation energy of single Zn defect in ZnO NWs

$$E_{\mathrm{f}} = E(\mathrm{ZnO})_{\mathrm{defect}} + n\mu_{\mathrm{Zn}} - E(\mathrm{ZnO})_{\mathrm{defect-free}}, \qquad (1)$$

where $E(\mathrm{ZnO})_{\mathrm{defect}}$ is the total energy of the single defect ZnO NW, $E(\mathrm{ZnO})_{\mathrm{defect-free}}$ denotes the total energy of the defect-free system, and μ_{Zn} is the chemical potential for Zn atom. To avoid the interaction between single Zn defect, a $1\times1\times2$ supercell is adopted in our calculations. As reported in Table 1, formation energies have the lowest value at the surface of the NW (namely, p3 position), where the formation energy is only 2.444 eV for bared ZnO NW. For the passivated ZnO NW, the most stable position is at p2 and the formation energy is equal to 2.571 eV. This conclusion agrees well with the general trends observed in Cu-doped GaN NW, i.e., the H passivation can affect the stability of the cationic defect.

The results shown in Table 1 also indicate that the ability of the single cationic defect formation depends sensitively on the surface termination of the ZnO NW.

Table 1. Relative formation energy ΔE of a single Zn defect in bared and passivated ZnO NWs.

Cation defect	Zn_{p1}	Zn_{p2}	Zn_{p3}
E_f(H + ZnO)/eV	2.752	2.571	3.137
E_f(ZnO)/eV	2.553	2.675	2.444

Moreover, we find that the defect-induced local magnetic moment is close to $2\mu_B$ in all cases with a single Zn defect in ZnO NW and the ZnO NW with O defect is nonmagnetic. This outcome reveals that the ferromagnetism in the ZnO NW is correlated directly with a Zn defect, which is also consist with the experimental results.[36,37] As shown in Figs. 2(a) and 2(b), the spin density has different behaviors in bared and H-passivatied ZnO NWs. For the bared NWs, the spin density is more delocalized, indicating that the surface states have strong effect on the spin distribution. Generally, a local magnetic moment is formed by the localized electrons. For bared ZnO NW, the calculated magnetic moment is $1.92\mu_B$, while $2.00\mu_B$ in H-passivatied case. The reduced magnetic moment suggests that defective states of Zn vacancy interact with the surface states of bared NWs.

To see how the surface and vacancies change the electronic structures, we plot the projected DOS (PDOS) for such systems. As shown in Figs. 3(a) and 3(b), without any surface modifications, the dangling bonds of the surface have contributed to the states around the Fermi level in bared NW, which disappears in H-passivatied case. By introducing a single Zn vacancy, we find that the PDOS almost keeps their original shape, except for the spin-polarized defect states around the Fermi level (Figs. 3(c) and 3(d)).

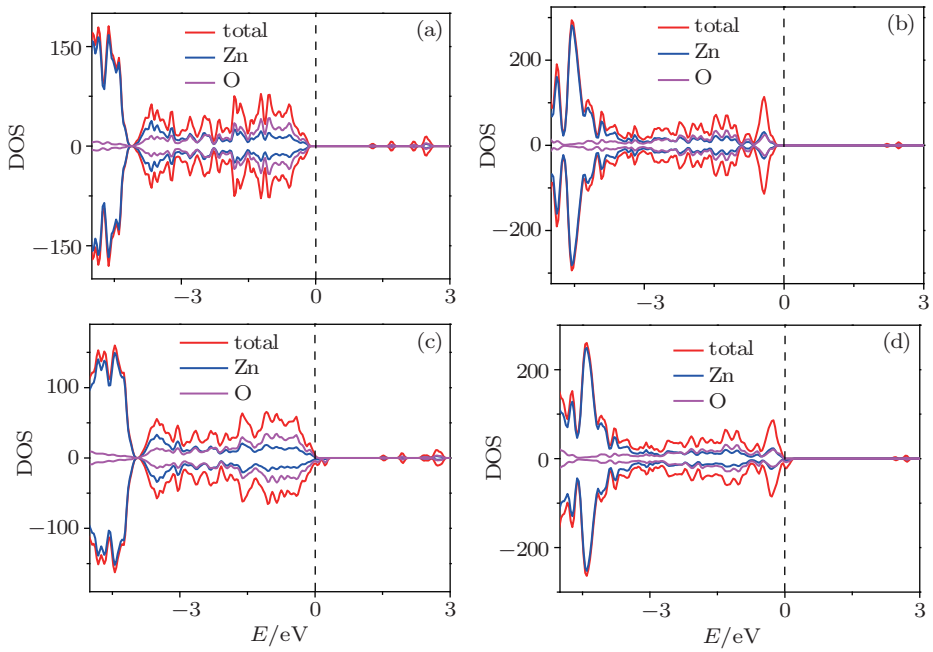


Fig. 3. (color online) Plotted DOS of ZnO NWs. The left column is DOS for the bared ZnO NWs and the right column is DOS for the passivated ZnO NWs. (a), (b) defect-free ZnO NW; (c), (d) single-defect ZnO NW.

It is well known that existence of the local magnetic moments does not necessarily result in collective magnetism. In order to study the magnetic interaction between these defect-induced local moments, we use the $1\times1\times4$ supercells containing two Zn defects separated by different distances varying from 4.566 Å to 18.601 Å. The magnetic interaction between the two defects in the ZnO NWs is studied through calculating the total energy of different spin states, that is, ferromagnetic (FM) and antiferromagnetic (AFM) states. The energy difference between the FM and AFM states versus the distance of the two Zn defects is presented in Fig. 4. For the bared ZnO NW, the spin interaction is determined by the distance of two vacancies. When the distance is less than 5 Å, local magnetic moments have strong spin interaction. As shown in Fig. 4, the energy difference is about 200 meV, which ensures that the magnetic structure can survive under room temperature. While for the longer distance, we can see that the local moments do not interact with each other, indicating the existence of a spin-glass state. On the other hand, for H-passivated NWs, we find that there is no strong spin interaction in any of the studied states. Consequently, the RFM cannot be obtained in H-passivated ZnO NW.

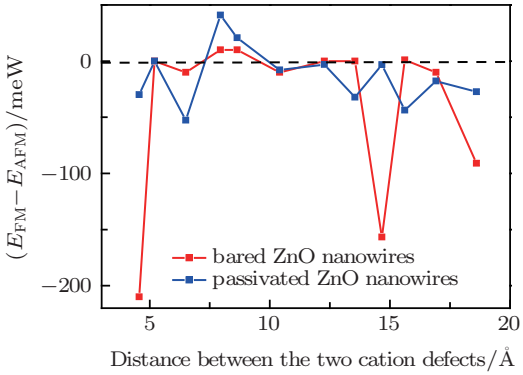


Fig. 4. (color online) Energy difference between the AFM and FM state for all possible inequivalent configurations of two Zn defects in a bared and passivated ZnO nanowires with 1×1×4 supercell.

As we know, the energy gap will be underestimated by the GGA method. However, the localization of Zn vacancies is still well described, as confirmed by the calculated magnetic moments ($1.92\mu_B$). Moreover, we have shown that the spin interaction has no connection with the position of conductive band. Therefore, we believe that the GGA method is reliable for the study of magnetic property of defective ZnO, as shown in previous reports.[19–24]

4. Conclusion

In summary, we systematically investigate the electronic structures, magnetic properties, and spin interaction in the ZnO nanowires via first-principle calculation. Our results indicate that single Zn vacancy in both bared and H-passivated ZnO NW can produce a local magnetic moment, which is close to $2\mu_B$. Since saturated hydrogen atoms remove the surface states of ZnO NWs, the spin interaction between two local magnetic moments is greatly reduced, leading to weak magnetic structure. However, for bared NW, the RFM can be obtained in the short distance of two Zn vacancies. Therefore, our results show that surface states are important for magnetic interaction in d^0 semiconductors, and should be kept in experiment to achieve RFM devices.

References

[1] Wolf S, Awschalom D, Buhrman R, Daughton J, Molnár S, Roukes M, Chtchelkanova A and Treger D 2001 *Science* **294** 1488
[2] Zunger A and Lany S 2010 *Physics* **3** 53
[3] Ohno H 1998 *Science* **281** 951
[4] Yamada Y, Ueno K, Fukumura T, Yuan H, Shimotani H, Iwasa Y, Gu L, Tsukimoto S, Ikuhara Y and Kawasaki M 2011 *Science* **332** 1065
[5] Jungwirth T, Sinova J, Mašek J, Kučera J and MacDonald A 2006 *Rev. Mod. Phys.* **78** 809
[6] Norton D, Pearton S, Hebard A, Theodoropoulou N, Boatner L and Wilson R 2003 *Appl. Phys. Lett.* **82** 239
[7] Dietl T, Ohno H, Matsukura F, Cibert J and Ferrand D 2000 *Science* **287** 1019
[8] Esquinazi P, Spemann D, Höhne R, Setzer A, Han K and Butz T 2003 *Phys. Rev. Lett.* **91** 227201
[9] Garcia M, Merino J, Fernández P E, Quesada A, Venta J, Ruíz González M, Castro G, Crespo P, Llopis J, González-Calbet M and Hernando A 2007 *Nano Lett.* **7** 1489
[10] Ohldag H, Tyliszczak T, Höhne R, Spemann D, Esquinazi P, Ungureanu M and Butz T 2007 *Phys. Rev. Lett.* **98** 187204
[11] Venkatesan M, Fitzgerald C and Coey J 2004 *Nature* **430** 630
[12] Zhu X and Su H 2009 *Phys. Rev. B* **79** 165401
[13] Wu H, Stroppa A, Sakong S, Picozzi S, Scheffler M and Kratzer P 2010 *Phys. Rev. Lett.* **105** 267203
[14] Das Pemmaraju C and Sanvito S 2005 *Phys. Rev. Lett.* **94** 217205
[15] Chan J, Lany S and Zunger A 2009 *Phys. Rev. Lett.* **103** 016404
[16] Xia H, Li W, Song Y, Yang X, Liu X, Zhao M, Xia Y, Song C, Wang T, Zhu D, Gong J and Zhu Z 2008 *Adv. Mater.* **20** 4679
[17] Pan H, Yi J, Shen L, Wu R, Yang L, Lin J, Feng Y, Ding Y, Van H and Yin J 2007 *Phys. Rev. Lett.* **99** 127201
[18] Song B, Bao H, Li H, Lei M, Peng T, Jian J, Liu J, Wang W and Chen X 2009 *J. Am. Chem. Soc.* **131** 1376
[19] Liu Y, Wang G, Wang S, Yang J, Chen L, Qin X, Song B, Wang B and Chen X 2011 *Phys. Rev. Lett.* **106** 087205
[20] Kan E, Wu F, Zhang Y, Xiang H, Lu R, Xiao C, Deng K and Su H 2012 *Appl. Phys. Lett.* **100** 072401
[21] Peng H, Xiang H, Wei S, Li S, Xia J and Li J 2009 *Phys. Rev. Lett.* **102** 017201
[22] Dev P, Xue Y and Zhang P 2008 *Phys. Rev. Lett.* **100** 117204
[23] Kan E, Wu F, Wu H, Xiao C, Xiang H and Deng K 2013 *Appl. Phys. Lett.* **102** 022422
[24] Xiang H and Wei S 2008 *Nano Lett.* **8** 1825
[25] Kim B and Kwon J 2014 *Sci. Rep.* **4** 4379
[26] Bai Y, Yu H, Li Z, Amal R, Lu G and Wang L 2012 *Adv. Mater.* **24** 5850
[27] Zhu R, Zhang W, Li C and Yang R 2013 *Nano Lett.* **13** 5171
[28] McCune M, Zhang W and Deng Y 2012 *Nano Lett.* **12** 3656
[29] Cha S, Jang J, Choi Y, Amaratunga A, Ho G, Welland M, Hasko D, Kang D and Kim J 2006 *Appl. Phys. Lett.* **89** 263102
[30] Bao J, Zimmler M, Capasso F, Wang X and Ren Z 2006 *Nano Lett.* **6** 1719
[31] Zhu G, Yang R, Wang S and Wang Z 2010 *Nano Lett.* **10** 3151
[32] Kresse G and Hafner J 1993 *Phys. Rev. B* **47** 558
[33] Perdew J and Wang Y 1992 *Phys. Rev. B* **45** 13244
[34] Kresse G and Furthmüller J 1996 *Comput. Mater. Sci.* **6** 15
[35] Kresse G and Furthmüller J 1996 *Phys. Rev. B* **54** 1169
[36] Li J, Jiang Y, Li Y, Yang D, Xu Y and Yan M 2013 *Appl. Phys. Lett.* **102** 072406
[37] Phan T, Zhang Y, Yang D, Nghia N, Thanh T and Yu S 2013 *Appl. Phys. Lett.* **102** 072408